Design and Implantation of an Engineered Porcine Accessory Carpal Osteochondral Unit

Brendan Stoeckl, MS[1, 2]
Hannah Zlotnick, BS[1, 2, 3]
Megan Farrell, PhD[1]
Liane Miller, MD[1, 2]
Thomas Schaer, VMD[4]
Michael Hast, PhD[1]
Robert Mauck, PhD[1, 2, 3]
David Steinberg, MD[1, 2]

1 Department of Orthopaedic Surgery, University of Pennsylvania, Philadelphia, PA

2 Translational Musculoskeletal Research Center, CMC VAMC, Philadelphia, PA

3 Department of Bioengineering, Philadelphia, PA

4 Comparative Orthopaedic Research Laboratory, School of Veterinary Medicine, Kennett Square, PA

Introduction

Trapeziometacarpal (TMC) osteoarthritis (OA) is one of the most common conditions affecting middle and older aged adults.[1] Conservative treatments often fail in the long term, and many patients will eventually require destructive surgical intervention, involving removal of all or part of the trapezium and replacement with tendon, fascia, or an artificial implant.[2] While effective at reducing pain, these procedures compromise grip strength and, in some cases, result in subsidence and disFigurement of the hand.[2] Efforts to replace articular cartilage (and bone) with living, functional tissue have matured substantially over the last two decades,[3] as has technology for generating constructs that can match the anatomical complexity and geometry of native articulating surfaces.[3,4] For these technologies to progress toward translation, appropriate large animal models are required. In our previous work, we identified the porcine accessory carpal (AC) as a potential model for TMC OA, given its similar shape, size, mechanics, and chemical composition, and we designed a tissue engineered implant for the articulating surface of the AC.[5, 6] Here, we further explore the loading patterns of this joint as a function of flexion, refine the design of our proposed implant, and evaluate the feasibility of its implantation in the Yucatan minipig forelimb.

Methods

CT images of the forelimb of a skeletally mature Yucatan minipig were obtained and 3D models of the bones were segmented in ITK-SNAP.[7] A musculoskeletal model was generated in OpenSim, and the relative motion of the AC and its contact forces were evaluated through passive range of motion. Three adult minipig forelimbs were obtained from unrelated studies. In each, an incision was made and a TekScan iScan 6900 pressure sensor was placed into joint space between the accessory carpal and the ulnar carpal. The carpus was moved through a range of angles from 90 degrees to full extension while contact forces were measured. To reduce the bony component of the implant while simultaneously increasing surface area for potential cell ingress and bony integration, our previous implant was redesigned. Two different surgical fixation designs were evaluated—a "cross" keel and a single "keel" design (Figure 1A). Simplified mock-ups of the cross keel and single keel fixation methods were created in Solidworks (Dassault Systèmes), and a finite element analysis was performed (Figure 1B). The keel was rigidly fixated and a 3N load was applied to the lateral face of the implant, with the materials assigned a bulk modulus of 3MPa. Positive molds of the keel design were 3D printed out of an ABS-like photopolymer (Figure 2B). To fabricate elastomeric negative molds, Sylgard 184 (polydimethylsiloxane, PDMS) was prepared at a 10 parts monomer to 1 part curing agent ratio, poured over the 3D printed designs, degassed, and allowed to cure at 40°C overnight. Poly(ε-caprolactone) (PCL) was dissolved in chloroform at 20% wt/vol and mixed with NaCl crystals sieved to ~106 μm, and Zirconium nanoparticles were included for radioopacity. The slurry was poured into the mold and the solvent was evaporated. The units were demolded and the salt was leached. We next performed a proof-of-concept surgery on an adult minipig forelimb. We made an incision

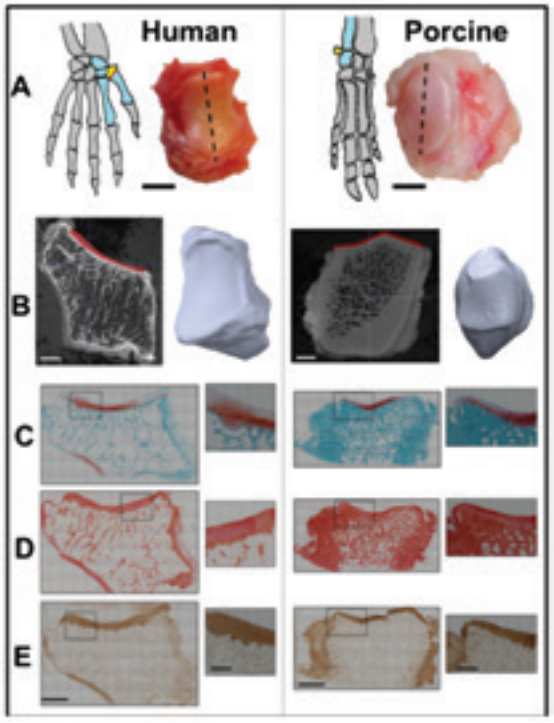

Figure 1. (A) Solidworks models of three different AC implant designs: peg, cross, and keel; **(B)** Finite element model of cross (top) and keel (bottom) implant designs. Von Mises stress is on the left and strain is on the right.

into the joint and rotated the articulating surface of the AC into view. We used a reciprocating saw followed by an osteotome to remove the surface of the AC and a 2mm burr followed by a curette to create a slot in the remaining bone, matching the keel on the implant. The construct was held in place with two 1mm Ø by 8mm long bicortical screws oriented normally to the plane of the keel. Fluoroscopy and MicroCT were performed to evaluate positioning of the implant. Images were segmented using ITK-SNAP and visualized in Meshlab (ISTI).

Results

In the OpenSim model, the contact force remained ~0 as the carpus was extended until ~20 degrees flexion. At this point, force increased and reached a peak of 67N at full extension (Figure 3C). In the *ex vivo* experiment (Figure 3D), the force across the joint remained close to zero until 15 degrees of flexion, and then rose rapidly to a maximum of 29.1±10.5N at 0 degrees (Figure 3E). The contact area and stress followed the same pattern (Figure 3F-G). The AC implant design from our previous work had a volume of 423 mm^3 and an integrating surface area of 129.3 mm^2. Two new designs—the cross keel and single keel, had volumes of 380.75mm^3 and 355.65mm^3 and integrating surface areas of 240.5mm^2 and 215.6mm^2, respectively (Figure 1A). FE modeling showed that the centroid of the implant displaced by 0.18 mm in the cross keel design and 0.22mm in the single keel design (Figure 1B). Neither experienced local strains over 7%. We chose the single keel design for implantation (Figure 2A). Using a 3D printed positive mold, we produced a PDMS negative mold (Figure 2B) which was used to create a porous PCL implant (Figure 2C). This was readily implanted into a cadaveric minipig forelimb (Figure 2D) and was visible fluoroscopically (Figure 2E) and on μCT (Figure 2F).

Discussion

In this study, we expanded on our previous work[5,6] by further characterizing the biomechanical environment

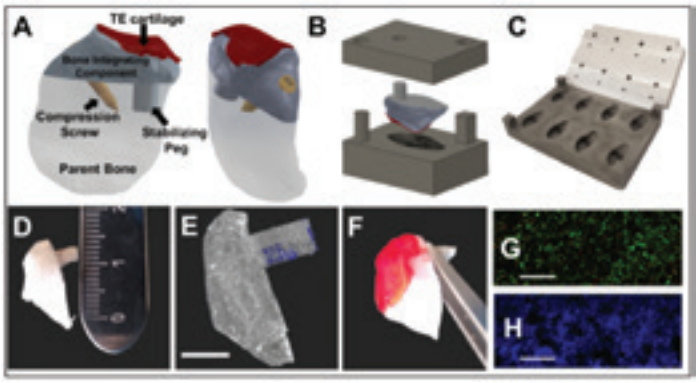

Figure 2. (A) Design of composite implant with keel, bicortical screws, parent bone, and TE cartilage surface (in red); **(B)** ABS positive mold (top) and PDMS negative mold (bottom) used to create PCL implant **(C)**; **(D)** Implantation of PCL construct; **(E)** Fluoroscopic visualization of implant *in situ*; **(F)** μCT and 3D rendering of AC implant *in situ*.

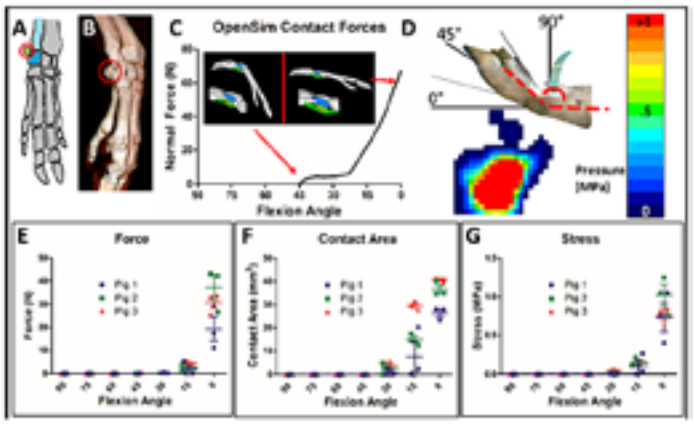

Figure 3. (A) Diagram of porcine AC (yellow) and its articulation with the ulnar carpal (blue) and ulna (light blue); **(B)** μCT rendering with AC identified; **(C)** Plot of contact forces computed in OpenSim model; **(D)** Example TekScan pressure map of the AC contact; **(E-G)** Plots of force, contact area, and stress with respect to flexion angle computed with TekScan.

experienced by the AC in the Yucatan minipig, refining the design of our implant, improving the fabrication process, and finally implanting an engineered AC into a minipig forelimb. The loading pattern measured *ex vivo* matched that predicted via OpenSim. These models and data show that the AC is essentially unloaded except when the carpus is fully extended. This means that when implanted into a living animal, the construct will only experience loads when the animal is standing, or in the stance phase of ambulation. We chose the single keel implant design because it offered a reduced volume to be filled in with bone, while increasing the surface area over which boney integration could occur. It was not appreciably less stable than the cross design in FE simulations, and practically speaking, allowed for a much easier surgical approach to implantation. Next steps are to evaluate the long-term function of a cell seeded osteochondral implant (with a stem cell-laden hydrogel cap to form a cartilage layer) in a living animal.

Significance

This study refined the design, fabrication, and implantation of an engineered porcine AC, furthering the goal of total biologic resurfacing of this joint as an analog for the treatment of TMC OA in humans.

References:

1. Becker et al., CORR, 2013.
2. Wajon et al., Cochrane Database, 2015.
3. O'Connell et al., J Knee Surg, 2012.
4. Saxena et al., Tissue Eng, 2016.
5. Stoeckl et al., ORS 2018.
6. Stoeckl et al., ORS 2019.
7. Yushkevich et al., Neuroimage, 2006.